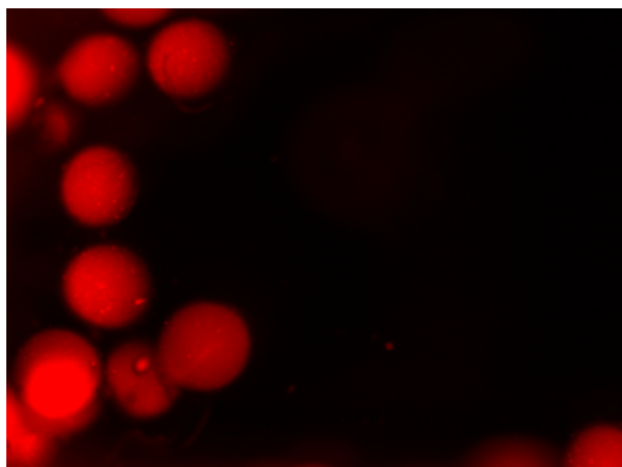


Supporting Information

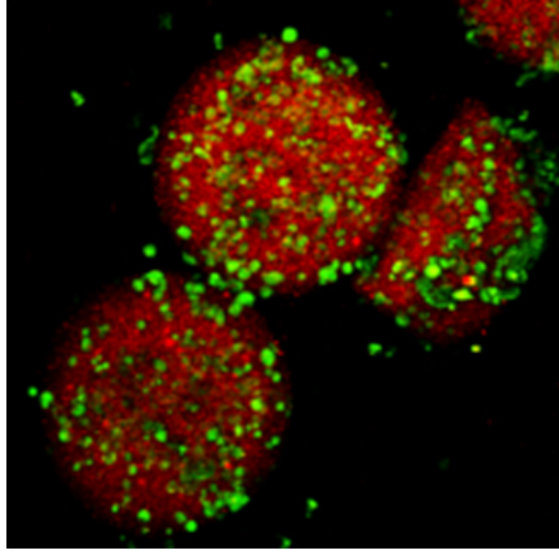
Supplemental Figures and Figure Captions



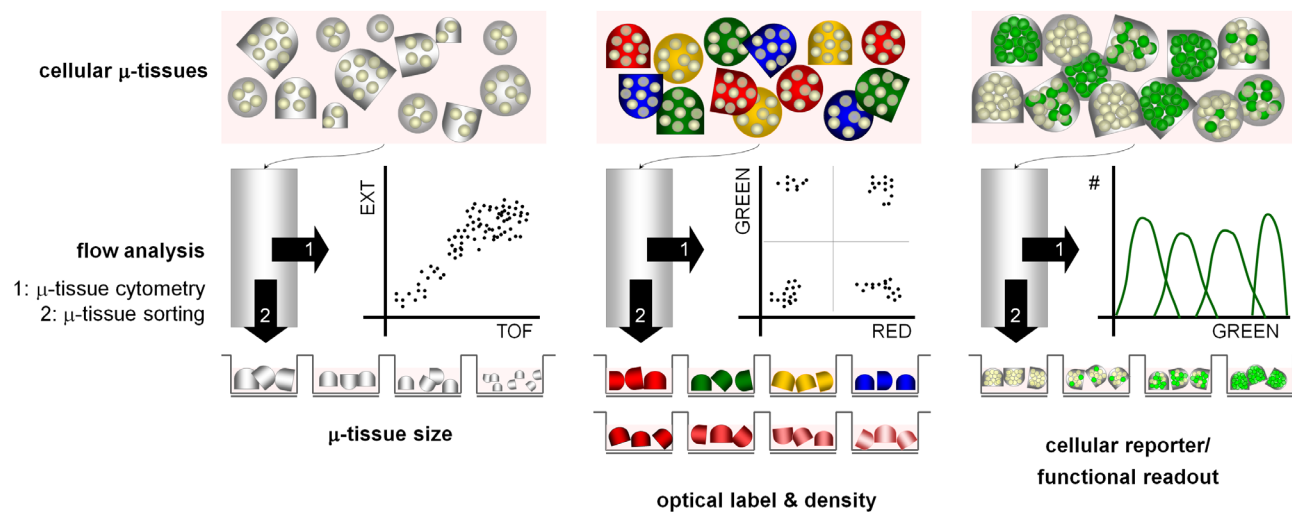
Supplemental Movie 1. 3D μ -tissue suspensions. 3D μ -tissues containing pre-assembly red quantum dot codes, manipulated by manual pipetting under a UV lamp.



Supplemental Movie 2. 3D μ -tissue suspensions in channel. 3D μ -tissues containing pre-assembly red quantum dot codes in a poly(dimethylsiloxane) (PDMS) microfluidic channel adhered to a glass coverslip, with flow driven by a syringe pump.

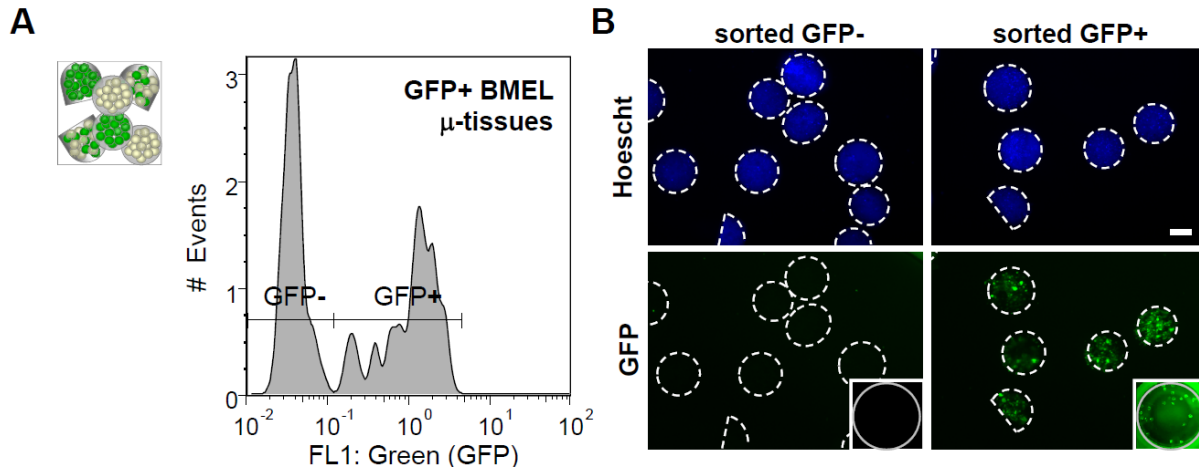


Supplemental Movie 3. Confocal imaging and 3D projection of engineered μ -tissues. 3D μ -tissues co-encapsulating BMEL cells and pre-assembly red quantum dot codes were incubated with the green calcein AM viability dye, then mounted using Fluoromount-G mounting medium (Southern Biotech) on a 35-mm glass bottom dish (Mattek) with a 22 cm² coverslip. Confocal z-stack images and 3D projections were acquired using a Zeiss Laser Scanning Microscope (LSM) 510 confocal microscope (W.M. Keck Microscopy Facility, Whitehead Institute) and accompanying LSM software.



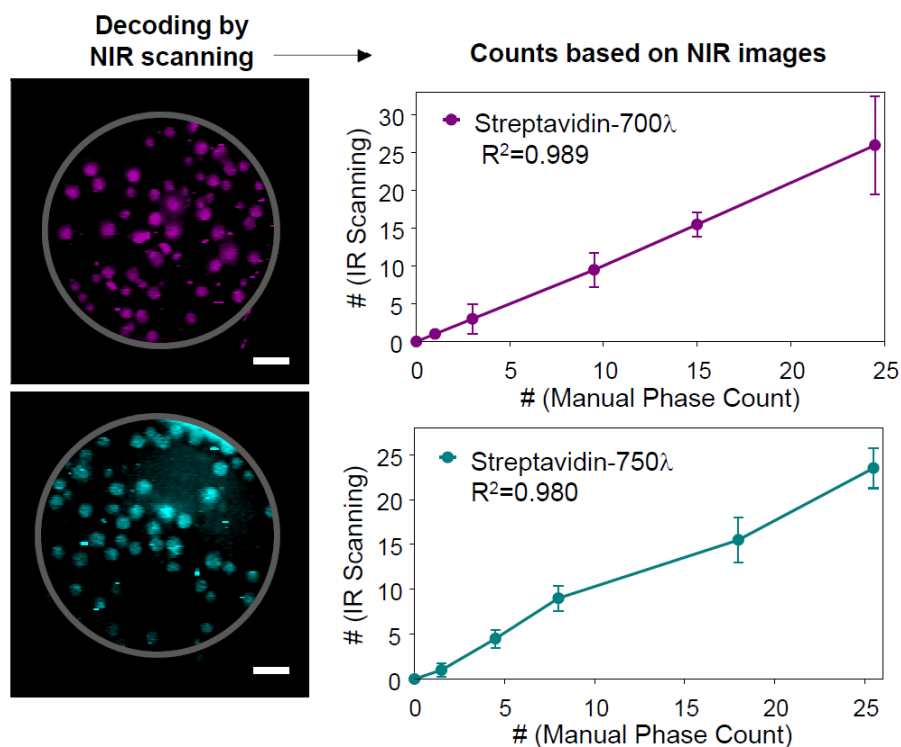
Supplemental Figure 1. Overview of μ -tissue cytometric analysis capabilities.

Schematic illustrating flow analysis and enrichment of μ -tissues based on multiple parameters. These include measurements of μ -tissue size (time-of-flight, TOF) and optical density (extinction, EXT), optical encoding for multiplexed parallel analysis, and fluorescent readouts of cellular gene expression and function.

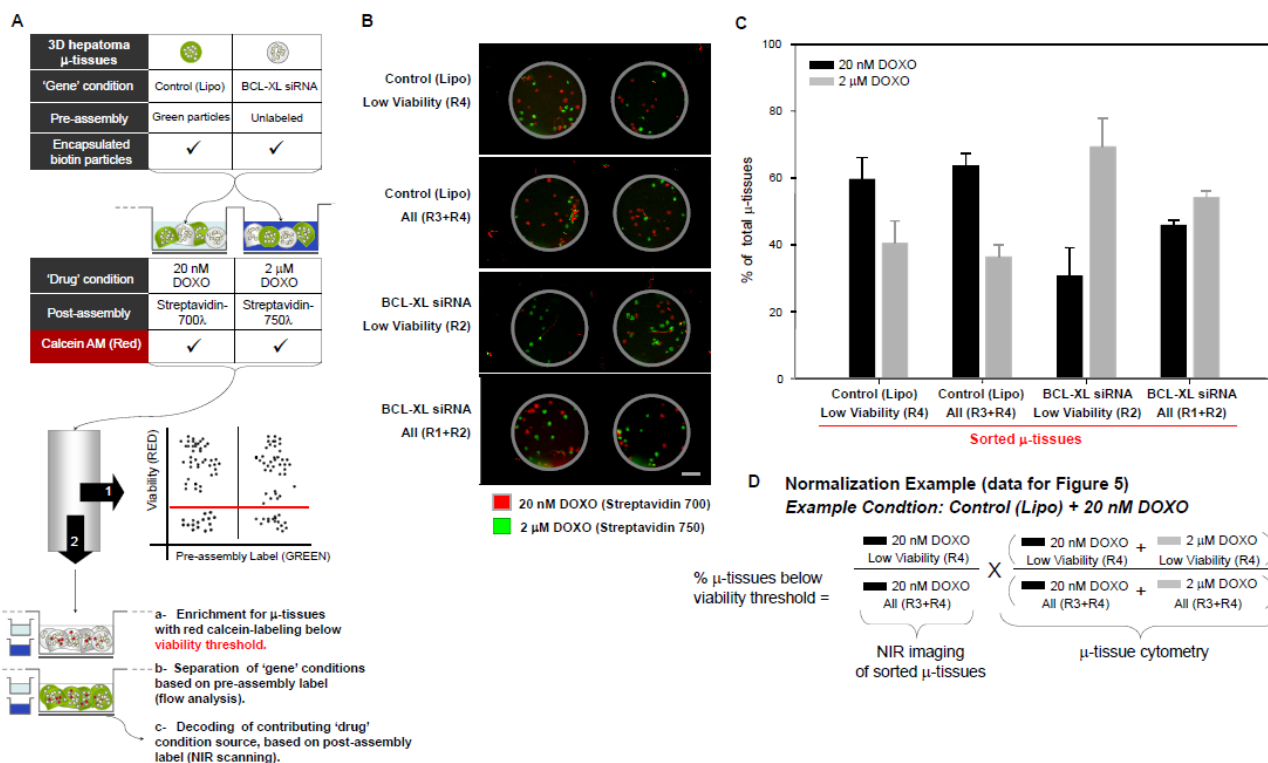


Supplemental Figure 2. Flow sorting progenitor μ -tissues with a fluorescent reporter.

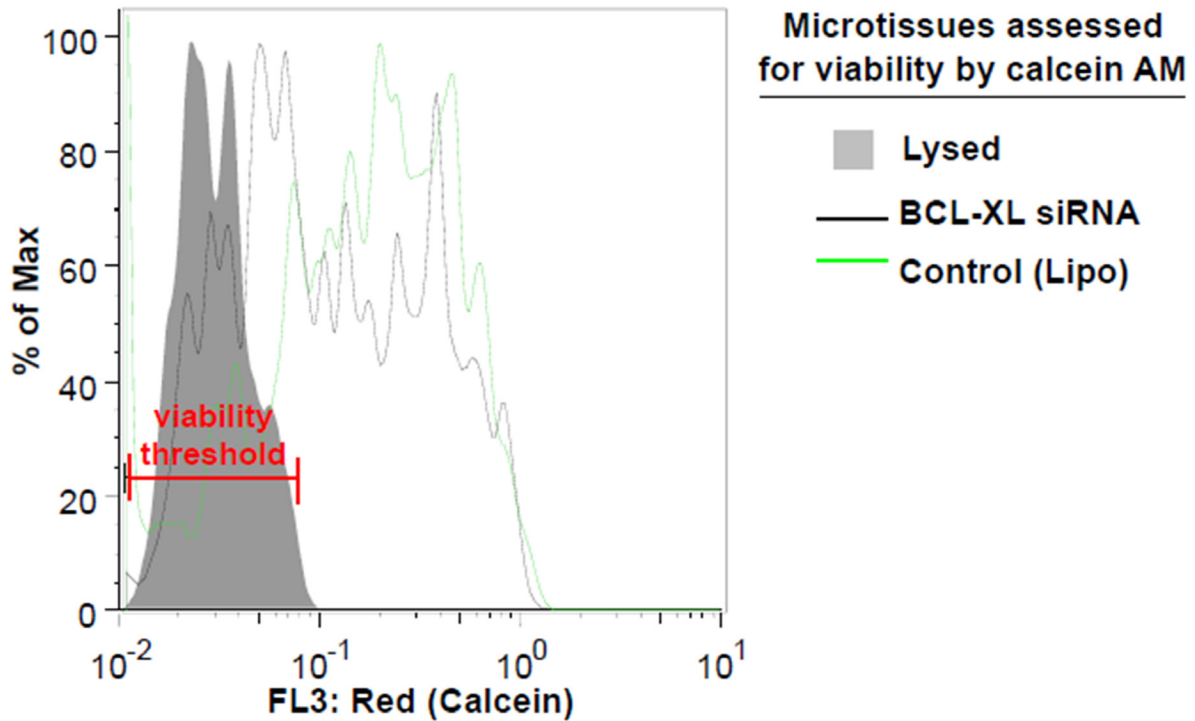
A) 3D BMEL μ -tissues and 3D GFP+ BMEL μ -tissues were mixed as shown in the schematic inset, then analyzed for reporter gene expression using flow cytometry ($n=278$ tissues). Compared to control BMEL μ -tissues, the mean fluorescence intensity of the GFP+ reporter μ -tissues population was measured as ~ 32 -fold higher. Fluorescence-activated sorting based on reporter expression enabled separation of GFP- and GFP+ μ -tissues. B) Representative epifluorescence micrographs of enriched GFP- and GFP+ μ -tissues sorted into a 96-well plate, and counterstained with Hoescht nuclear stain. The inset shows a lower magnification image of the entire 30 cm^2 well area. (Scale bar, 200 μm .)



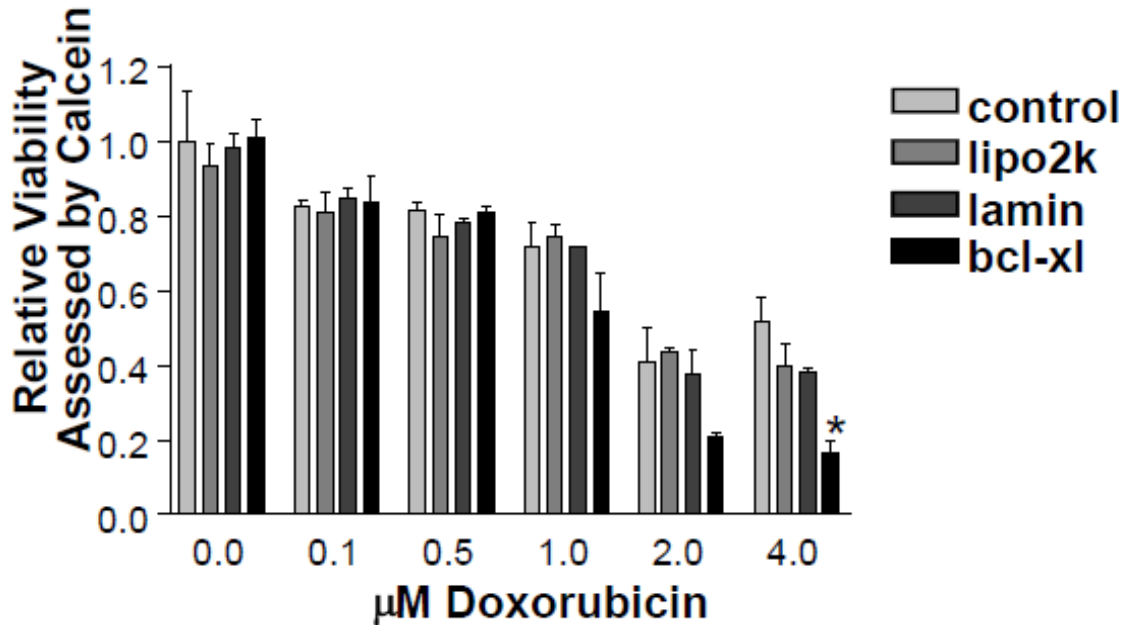
Supplemental Figure 3. Near infrared (NIR) scanning and quantification of post-assembly (*post-hoc*) labeled μ -tissues. Post-assembly (*post-hoc*) labeled μ -tissues in a 96-well plate were imaged using the Odyssey IR imaging system (LI-COR) at a scanning resolution of 42 μ m. NIR scanning demonstrates diffusion and retention of the solution NIR code, and counts based on decoded images enable quantification. Linear regression analysis confirmed a strong positive correlation between representative counts from decoded IR images and manual counts from phase images ($R^2=0.989$ for $\lambda=700$, $R^2=0.980$ for $\lambda=800$). Error bars represent s.d. of the mean ($n=2$). (Scale bar, 1 mm.)



Supplemental Figure 4. Multiplex encoding of gene knockdown and drug treatment, and quantified effects of combination therapy on 3D hepatoma μ -tissue viability. A) Experimental design and schematic of multiplexing experiment. 3D hepatoma μ -tissues subject to different 'gene' conditions were fabricated by encapsulating control (Lipofectamine-treated) or BCL-XL siRNA-treated HepG2 cells, along with pre-assembly green particle or unlabeled tags. The μ -tissues were also fabricated to contain biotin particle templates for *post-hoc* reaction with different 'drug' solutions, 20 nM or 2 μ M doxorubicin (DOXO), containing post-assembly streptavidin-NIR soluble labels (700 λ or 750 λ). Multiplexed μ -tissue mixtures were pooled and collectively stained with the red calcein AM live dye. Using cytometric analysis, μ -tissues were assessed simultaneously for pre-assembly code identification (green fluorescence) and viability (red fluorescence) (1), and fluorescence-activated sorted for μ -tissue 'responders' with viability below a threshold defined by non-viable controls (red line) (2). Post-assembly, *post-hoc* codes were later resolved using NIR scanning to quantify μ -tissue exposure. B) High resolution (42 μ m) NIR scans of a 96-well plate following flow-activated analysis and sorting for μ -tissue 'responders' (Low Viability), and general μ -tissue population samples (All). Sorting criteria is denoted by gates R1, R2, R3 and R4 depicted in Figure 5B. C) Count data from NIR scans of sorted μ -tissues, represented as % of total μ tissues. D) Quantification example, depicting how data from NIR scans and data from μ -tissue cytometry plot are formulated to define the "% μ -tissues below viability threshold" value for each combination of DOXO \pm siRNA treatment. (Scale bar, 1 mm.)



Supplemental Figure 5. Determination of viability threshold for identifying μ -tissue ‘responders’ to gene knockdown versus drug treatment or combined therapies. Flow histogram of red fluorescence depicts intensity of red calcein AM staining in different 3D hepatoma μ -tissue populations (control μ -tissues, BCL-XL siRNA-treated μ -tissues, and control μ -tissues incubated in lysis buffer). The “viability threshold” was set by gating for the lysed, least viable μ -tissue population, and this threshold was subsequently used to identify within flow cytometric plots the μ -tissue events with the greatest response to therapy (lowest viability).



Supplemental Figure 6. Synergy between drug treatment and siRNA-mediated knockdown.

To test the effect of doxorubicin and BCL-XL gene knockdown on HepG2 cells in a 2D multiwell format, HepG2 cells were seeded at 7,500 cells/well in a 96-well plate and cultured for 24h prior to siRNA transfection. Cells were transfected with 100 nM BCL-XL ON-TARGET plus SMARTpool siRNA (NM_001191, Dharmacon) or 100 nM Lamin A siRNA (NM_019290, Ambion), using Lipofectamine RNAi max (Invitrogen) according to manufacturer's instructions. Twenty-four hours following transfection, cells were dosed daily for 2d with doxorubicin HCl (0, 0.1, 0.5, 1.0, 2.0, 4.0 μM, Sigma). Viability was assessed utilizing green calcein AM labeling and fluorimetry (485/530 nm ex/em). Error bars represent s.d. of the mean ($n=2$). Statistical significance was determined using one-way ANOVA followed by Tukey's multiple comparison test (* $p<0.01$, relative to control/4.0 μM doxorubicin sample, $p<0.05$ relative to all other conditions treated with 4.0 μM doxorubicin).